Evident $PM_{2.5}$ Drops in the East of China due to the COVID-19 Quarantines in February

Zhicong Yin [123], Yijia Zhang[1], Huijun Wang[123], Yuyan Li[1]

[1]Key Laboratory of Meteorological Disaster, Ministry of Education / Joint International Research Laboratory of Climate and Environment Change (ILCEC) / Collaborative Innovation Center on Forecast and Evaluation of Meteorological Disasters (CIC-FEMD), Nanjing University of Information Science & Technology, Nanjing, 210044, China

[2]Southern Marine Science and Engineering Guangdong Laboratory (Zhuhai), Zhuhai, 519080, China

[3]Nansen-Zhu International Research Centre, Institute of Atmospheric Physics, Chinese Academy of Sciences, Beijing, China

Correspondence to: Zhicong Yin (yinzhc@163.com)

Abstract. The top-level emergency response to the COVID-19 pandemic involved an exhaustive quarantine in China. The impacts of COVID-19 quarantine on the decline in fine particulate matter ($PM_{2.5}$) were quantitatively assessed based on numerical simulations and observations in February. Relative to both of February 2017 and climate mean, anomalous southerlies and moister air occurred in the east of China in February 2020, which caused considerable $PM_{2.5}$ anomalies. Thus, it is a must to disentangle the contributions of stable meteorology from the effects of the COVID-19 lockdown. The contributions of routine emission reductions were also quantitatively extrapolated. The top-level emergency response substantially alleviated the level of haze pollution in the east of China. Although climate variability elevated the $PM_{2.5}$ by 29% (relative to 2020 observations), 59% decline related to COVID-19 pandemic and 20% decline from the expected pollution regulation dramatically exceeded the former in North China. The COVID-19 quarantine measures decreased the $PM_{2.5}$ in Yangtze River Delta by 72%. In Hubei Province where most pneumonia cases were confirmed, the impact of total emission reduction (72%) evidently exceeded the rising percentage of $PM_{2.5}$ driven by meteorology (13%).

Keywords: COVID-19, $PM_{2.5}$, Emission Reduction, Climate Variability, Haze

1 Introduction

The COVID-19 pandemic devastatingly blew China in the beginning of 2020 (Luo, 2020; Xia et al., 2020; Cao et al., 2020). By April 2020, more than 84 thousand confirmed cases were reported by the National Health Commission of China, approximately 75% of which were confirmed in February (Fig. 1a). To effectively control the large spread of COVID-19 pneumonia, stringent quarantine measures were implemented by the Chinese government and people themselves, including prohibiting social activities, shuttering industries, stopping transportation, etc. (Chen S. et al., 2020). The abovementioned emergency response measures were first carried out in Wuhan on 23 January, which resulted in the delayed arrival of COVID-19 in other cities by 2.91 days, and these response measures were in effect in all cities across China, thus limiting the spread of the COVID-19 epidemic in China (Tian et al., 2020). Since March 7, the number of newly confirmed cases in China has

been nearly below 100. On the other hand, the COVID-19 quarantine measures greatly reduced anthropogenic emissions, and therefore, the air quality in China was considerably improved (Wang et al., 2020). Chen K. et al. (2020) simply compared observations of atmospheric components before and during the quarantine and found that the concentration of fine particulate matter ($PM_{2.5}$) in Wuhan decreased 1.4 μg/m^3, but it decreased 18.9 μg/m^3 in 367 cities across China. Shi et al. (2020) quantified a 35% reduction of $PM_{2.5}$ on average during the COVID-19 outbreak compared to the pre-COVID-19 period. Huang et al. (2020) used comprehensive measurements and modeling to show that the haze during COVID-19 lockdown was driven by enhancements of secondary pollution, which offset reduction of primary emissions during this period in China. However, the impacts of meteorology on the air quality were neglected in many previous studies.

Climate variability notably influences the formation and intensity of haze pollution in China (Yin and Wang 2016; Xiao et al., 2015; Zou et al., 2017), and the impacts are embodied by variations in surface wind, boundary layer height and moisture conditions (Shi et al., 2019; Niu et al., 2010; Ding et al., 2014). During December 16th-21st 2016, although most aggressive control measures for anthropogenic emissions were implemented, severe haze pollution with $PM_{2.5}$ concentrations ≈ 1100μg m^{-3} still occurred and covered 710,000km^2. The continuous low surface wind speed of less than 2ms^{-1}, high humidity above 80% and strong temperature inversion lasting for 132h caused the rebound of wintertime $PM_{2.5}$ in 2016 (Yin and Wang, 2017). In winter 2017, the air quality in North China largely improved; however, the stagnant atmosphere in 2018 resulted in a major $PM_{2.5}$ rebound by weakening transport dispersion and enhancing the chemical production of secondary aerosols (Yin and Zhang 2020). Wang et al. (2020) applied the Community Multiscale Air Quality model to emphasize that the role of adverse meteorological conditions cannot be neglected even during the COVID-19 outbreak. From February 8 to 13 2020, North China suffered severe pollutions, with maximum daily $PM_{2.5}$ exceeding 200μg m^{-3}. During this period, weak southerly surface winds lasted for nearly 5 days, relative humidity was close to 100%, and atmospheric inversion reached more than 10°C. Although pollution emissions from basic social activities have been reduced, heavy pollution still occurred when adverse meteorological conditions characterized by stable air masses appeared (Wang et al., 2020).

After the severe haze events of 2013, routine emission reductions resulted in an approximately 42% decrease in the annual mean $PM_{2.5}$ concentration between 2013 and 2018 in China (Cleaner air for China, 2019). In November 2019, the Ministry of Environmental Protection of China issued a series of Autumn-Winter Air Pollution Prevention and Management Plans indicating that the routine emission reductions would be conventionally implemented in the following winter (Ministry of Environmental Protection of China, 2019). As reported by the government, the mean ratio of work resumption in large industrial enterprises was approximately 90% in the east of China until the end of February (Fig. 1b). In this study, we attempted to quantify the impacts of the COVID-19 pandemic on the observed $PM_{2.5}$ concentration in February 2020 when the quarantine measures were the strictest. The official 7-day Chinese New Year holiday occurs in January and February and commonly accounts for approximately 25% of a month. From 2013–2020, there were only two years (2017 and 2020) when the official 7-day holiday occurred in January (Fig. 1c). Thus, to avoid the impacts of the Spring Festival, the observed $PM_{2.5}$ concentration

in February 2017 (Fig. 1a) was adopted to calculate the $PM_{2.5}$ difference, which was decomposed into the results due to expected routine emission reductions, changing meteorology climate variability, and COVID-19 quarantines.

2 Datasets and methods

2.1 Data description

Monthly mean meteorological data from 2015 to 2020 were obtained from NCEP/NCAR reanalysis datasets, with a horizontal resolution of 2.5°×2.5°, including the geopotential height at 500 hPa (H500), zonal and meridional winds at 850 hPa, vertical wind from the surface to 150 hPa, and relative humidity at the surface (Kalnay et al., 1996). $PM_{2.5}$ concentration data from 2015 to 2020 were acquired from the China National Environmental Monitoring Centre (https://quotsoft.net/air/). The monitoring network expanded from 1500 sites in 2015 to 1640 sites in 2020, covering approximately 370 cities nationwide. The $PM_{2.5}$ data were monitored every 5 min using two methods: a tapered element oscillating microbalance and β-rays, which were operated under the China National Quality Control.

2.2 GEOS-Chem description, evaluation and experimental design.

We used the GEOS-Chem model (http://acmg.seas.harvard.edu/geos/) to simulate the $PM_{2.5}$ concentration, driven by MERRA-2 assimilated meteorological data (Gelaro et al., 2017). The nested grid over China (15° N–55° N, 75–135° E) had a horizontal resolution of 0.5° latitude by 0.625° longitude and consisted of 47 vertical layers up to 0.01 hPa. The GEOS-Chem model included the fully coupled O_3–NO_x–hydrocarbon and aerosol chemistry module with more than 80 species and 300 reactions (Bey et al., 2001; Park et al., 2004). The $PM_{2.5}$ components simulated in the GEOS-Chem model included sulfate, nitrate, ammonium, black carbon and primary organic carbon, mineral dust, and sea salt. Aerosol thermodynamic equilibrium is computed by the ISORROPIA package, which calculates the gas–aerosol partitioning of the sulfate–nitrate–ammonium system (Fountoukis and Nenes, 2007). Heterogeneous reactions of aerosols include the uptake of HO_2 by aerosols (Thornton et al., 2008), irreversible absorption of NO_2 and NO_3 on wet aerosols (Jacob, 2000), and hydrolysis of N_2O_5 (Evans and Jacob, 2005). Two alternate simulations of aerosol microphysics are implemented in GEOS-Chem: the TOMAS simulation (Kodros and Pierce, 2017) and the APM simulation (Yu and Luo, 2009).

GEOS-Chem model has been widely used to examine the historical changes in air quality in China and quantitatively separate the impacts of physical-chemical processes. Using the GEOS-Chem model, Yang et al. (2016) found an increasing trend of winter $PM_{2.5}$ concentrations during 1985–2005, 80% of which due to anthropogenic emissions and 20% due to meteorological conditions. Here, we simulated the $PM_{2.5}$ concentrations in February 2017 and evaluated the performance of GEOS-Chem (Fig. S1a). The values of mean square error / mean equals were 5.8%, 7.0% and 5.4% in North China (NC), Yangtze River Delta (YRD) and Hubei Province (HB), respectively, indicating the good performance of reproducing the haze-

polluted conditions. The absolute biases were larger in the south of China, which was consistent with Dang and Liao (2019). They also compared the simulated and observed daily mean $PM_{2.5}$ concentrations at the Beijing, Shanghai, and Chengdu grids, which had a low bias in Beijing and high biases in Shanghai and Chengdu, respectively. The simulated biases possibly affected the subsequent results and brought uncertainties to some extent. The simulated spatial distribution of $PM_{2.5}$ was also similar to that of observations with spatial correlation coefficient = 0.78. We further verified whether the simulations could capture the roles of meteorological changes in February 2020 under a substantial reduction in emissions because of COVID-19 quarantines. In NC, YRD and HB, the correlation coefficients between daily $PM_{2.5}$ observations and simulated data under 2010 (1985) emission scenario reached 0.83 (0.82), 0.67 (0.63), and 0.79 (0.73), respectively. For example, in NC, the simulation could well simulate severe haze events (e.g., from 8–13 and 19–25 February) and good air quality events (e.g., from 14–18 February), reflecting that it has ability to accurately capture the change of meteorological conditions (Fig. S1b).

The $PM_{2.5}$ concentration in February from 2015 to 2020 was simulated in this study. Due to delayed updates of the emission inventory, we used the emissions data of 2010 (http://geoschemdata.computecanada.ca/ExtData/HEMCO/AnnualScalar) and 1985 (M. Li et al., 2017) for the simulations, which represented high- and low-emission scenarios, respectively. In total, we conducted two sets of numerical experiments to drive the GEOS-Chem simulations, one combining the meteorological conditions from 2015 to 2020 with fixed emissions in 1985 and the other with fixed emissions in 2010, which could determine the stability of simulated results.

2.3 The method to quantify the influence of the COVID-19 quarantine.

As mentioned above, we aimed to examine the impact of the COVID-19 quarantines on $PM_{2.5}$ over the February 2017 level basing on an observational-numerical hybrid method. The observed $PM_{2.5}$ difference in February 2020 (PMd_{OBS}) was linearly decomposed into three parts: the impacts of changing meteorology (PMd_M), expected routine emissions reductions (PMd_R) and COVID-19 quarantines (PMd_C), which was a reasonable approximation, and the decomposition equation was $PMd_{OBS} = PMd_M + PMd_R + PMd_C$. That is, $PMd_C = PMd_{OBS} – PMd_M – PMd_R$. It should be noted that PMd_C is the impact of the COVID-19 quarantines over the situation whereby the pandemic did not occur and routine emission reductions conventionally were in effect. The value of PMd_E (i.e., $PMd_R + PMd_C$) was the total impact of the emission reductions in February 2020 over the 2017 level.

Simulated $PM_{2.5}$ data driven by changing meteorology with two fixed-emissions (1985 and 2010) were employed to determine the ratio of PMd_M of each year/ observed $PM_{2.5}$ in 2017. Depending on the GEOS-Chem simulations, we found that the percentage of changed $PM_{2.5}$ due to the differences in meteorology remained nearly constant regardless of the emission level (Fig. S2), which was consistent with the results of Yin and Zhang (2020). This percentage was the difference of simulated $PM_{2.5}$ between each year and 2017 under the same emission scenario divided by the simulated $PM_{2.5}$ in 2017. For example, the percentages due to different meteorology between 2020 and 2017 were 22.1% (21.4%), –1.2% (–0.7%) and 9.0% (8.2%) in

NC, YRD and HB under the low (high) emissions (Fig. S2). The percentage under 2010 emission scenario was selected as the final percentage because the emissions from each sector in 2010 were more similar to recent years, and thus was more reasonable. Then, through multiplying the 2017 observation by this percentage , PMd_M can be quantified in each simulation grid with respect to 2017 (STEP 1).

From 2015 to 2019, $PMd_C = 0$; thus, $PMd_R = PMd_{OBS} - PMd_M$. Here, we repeated STEP 1 to determine PMd_M in each year from 2015 to 2019 relative to 2017 (i.e., $PMd_M = 0$ in 2017). After removing the effect of meteorological conditions in $PM_{2.5}$ differences, PMd_R in all years except 2020 can also be calculated. According to many previous studies, the change in emissions resulted in a linear change in air pollution in China from 2013-2019 (Wang et al., 2020; Geng et al., 2020) which might be related to the huge emission reduction due to the implementation of clean air action. Because the signal of emissions reduction in China had been particularly strong since 2013, it could be easily detected and the assumption of a linear reduction in pollution caused by emission reduction was applicable in China in the past few years. Based on this approximation, we used the method of extrapolation to speculate the impact of routine emission reduction on $PM_{2.5}$. We performed linear extrapolation based on known PMd_R values from 2015 to 2019 to obtain PMd_R in 2020 (STEP 2, Fig. S3). This PMd_R in 2020was calculated as the change of $PM_{2.5}$ caused by expected routine emission reduction, which did not actually happen, but merely gave an assessment in the case of "if no COVID-19". In Beijing and Shanghai, for example, $PM_{2.5}$ fell by 23.1% and 26.6% due to routine emission reduction in 2019, respectively, compared with 2015. Zhou et al. (2020) indicated that emission reductions caused 20–26% decreases in winter in Beijing which has been translated into 5 years. Zhang et al. (2020) also showed that the emission controls in Beijing-Tianjin-Hebei (BTH) region have led to significant reductions in $PM_{2.5}$ from 2013 to 2017 of approximately 20 % after excluding the impacts of meteorology. Geng et al. (2020) found a 20% drop in the main component of $PM_{2.5}$ in the Yangtze River Delta from 2013 to 2017. These results are consistent with our extrapolated results. Therefore, it is reasonable to obtain PMd_R by extrapolation after disentangling the effects of meteorological conditions.

Through STEP 1 and STEP 2, PMd_C and PMd_R, respectively, in 2020 can be determined. PMd_{OBS} can be directly calculated from the observed data. After removing the influences of climate anomalies and routine emission reductions, the impact of COVID-19 quarantines on $PM_{2.5}$ (PMd_C) was extracted as $PMd_{OBS} - PMd_M - PMd_R$ (STEP 3).

3 Results

The mean $PM_{2.5}$ concentration in February 2020 was nearly below 80 $\mu g/m^3$ at the vast majority of sites in the east of China, which was much lower than before (Fig. S4). North China (NC) was still the most polluted region (>40 $\mu g/m^3$), but the $PM_{2.5}$ concentrations in the Pearl River Delta (PRD) and Yangtze River Delta (YRD) were < 20 $\mu g/m^3$ and < 40 $\mu g/m^3$, respectively. Relative to the observations in February 2017, negative $PM_{2.5}$ anomalies were centered in NC, with values of approximately –60 to –40 $\mu g/m^3$ in southern Hebei Province and northern Henan Province (Fig. 2). In Hubei Province (HB),

where the COVID-19 pneumonia cases were the most severe in February, the $PM_{2.5}$ concentration was 20~40 μg/m^3 lower than that in 2017. The $PM_{2.5}$ differences were also negative in YRD and PRD. Therefore, how much did air pollution decrease due to the COVID-19 quarantines in February in east of China?

Climate variability notably influences the interannual-decadal variations in haze pollution as verified by both observational analysis (Yin et al., 2015) and GEOS-Chem simulations (Dang and Liao, 2019). Furthermore, Zhang et al. (2020) reported that meteorology contributes 50% and 78% of the wintertime $PM_{2.5}$ reduction between 2017 and 2013 in the BTH and YRD, respectively. Therefore, it is necessary to disentangle the influences of climate anomalies before quantifying the contributions of the COVID-19 quarantines on the air quality. The highest observed $PM_{2.5}$ concentrations were 274, 223, and 303 μg/m^3 in Beijing, Tianjin and Shijiazhuang, respectively. Although human activities had sharply decreased, severe haze pollution (e.g., 8–13 and 19–25 February 2020) was not avoided, which was attributed to the stagnant atmosphere (Wang et al., 2020), and these severe haze events were also reproduced by the GEOS-Chem simulation (see Section 2.2 and Fig. S1b).

As shown in Figure 4a-b, the meteorological conditions in February 2020 were more favorable for the occurrence of haze pollution in NC. In the mid-troposphere, an anomalous anticyclone was located over NC and the Sea of Japan (Fig. 4a). These anticyclonic anomalies clearly stimulated anomalous southerlies over eastern China, which not only transported sufficient water vapor to NC but also overwhelmed the climatic northerlies in winter (Fig. 4b). In addition, the anomalous upward motion associated with anomalous anticyclones prevented the downward transportation of westerly momentum and preserved the thermal inversion layer over NC (Fig. S5). Particularly, in the stagnant days (i.e., 8–13 and 19–25 February), the East Asia deep trough, one of the most significant zonally asymmetric circulations in the wintertime Northern Hemisphere (Song et al., 2016), shifted eastwards and northwards than climate mean, which steered the cold air to North Pacific instead of North China (Fig. 4c). The climatic northerlies in February, related to East Asia winter monsoon, also turned to be south winds in the east of China (Fig. 4d). Physically, the weakening surface winds and strong thermal inversion corresponded to weaker dispersion conditions, and the higher humidity indicated a favorable environment for the hygroscopic growth of aerosol particles to evidently decrease the visibility. Compared with the climate (February 2017) monthly mean, boundary layer height (BLH) decreased by 19.5m (34.5m), surface relative humidity (rhum) increased by 5% (10.6%) and surface air temperature (SAT) rose by 1.6°C (0.9°C) after detrending, which were conductive to the increase of $PM_{2.5}$ concentration in February 2020. Furthermore, the correlation coefficients of daily $PM_{2.5}$ and BLH, rhum, wind speed and SAT in North China were -0.63, 0.44, -0.45 and 0.46, respectively, all of which passed the 95% significance test and indicated importance of meteorology. We used the meteorological data in February 2017 to establish a multiple linear regression equation to fit $PM_{2.5}$. The correlation coefficients between the fitting results and the observed $PM_{2.5}$ concentration in NC, YRD and HB reached 0.84, 0.64 and 0.65, exceeding the 99% significance test. Then, we put the observed meteorological data in February 2020 into this established multiple regression equation to get the predicted $PM_{2.5}$ concentration. Using the regress-predicted value, the percentage of changed $PM_{2.5}$ due to the differences in meteorology between 2017 and 2020 were re-calculated and is 20.7%, -3.2% and 9.5%

in NC, YRD and HB, respectively (Fig. S2), which is consistent with and enhanced the robustness of the results obtained by our previous model simulation. Based on the GEOS-Chem simulations, PMd_M was calculated between February 2020 and 2017 (see Methods). To the south of 30°N, most PMd_M values were negative with small absolute values, at < 10 μg/m^3. To the north of 30°N, the PMd_M values were mostly positive, ranging from 30~60 μg/m^3 in BTH (Fig. 3a).

Since 2013, the Chinese government has legislated and implemented stringent air pollution prevention and management policies that have clearly contributed to air quality improvement (Wang et al., 2019). As mentioned above, without the COVID-19 pandemic, these emission reduction policies would certainly remain in effect in February 2020. Thus, we extrapolated PMd_R (i.e., the $PM_{2.5}$ difference due to expected routine emission reductions) between February 2020 and 2017 to isolate the impacts of the COVID-19 quarantines (i.e., PMd_C). PMd_R was mostly negative in the east of China (Fig. 3b). Because the impacts of meteorology were proactively removed, these negative values illustrated that routine emission reductions substantially reduced the wintertime $PM_{2.5}$ concentration. The contributions of the emission reduction policies were the greatest in the south of BTH and were also remarkable in Hubei Province (Fig. 3b). Although the PMd_R of Beijing in 2016 did not strictly comply with the pattern of monotonous decrease, which might be caused by the fluctuation of policy and its implementation, the value of PMd_R in 2020 relative to 2017 was –8.4 μg/m^3 and was comparable to the 11.5 μg/m^3 reductions due to policy during 2013–2017 (Zhang et al., 2020). In Shanghai, PMd_R was –12.0 μg/m^3 (Fig. 5), whose magnitude was proportional with assessments by Zhang et al. (2020), and the trend was nearly linear. The rationality of the extrapolations of PMd_R was also proved in Section 2.3. The trend of PMd_R in Wuhan was –9.6 μg/m^3 per year from 2015–2019, which indicated high efficiency of the emission reduction policies and resulted in large PMd_R values in 2020 (i.e., –21.8 μg/m^3).

By disentangling the impacts of meteorology and routine emission reduction policies, the change in $PM_{2.5}$ due to the COVID-19 quarantines was quantitatively extracted. As expected, this severe pandemic caused dramatic slumps in the $PM_{2.5}$ concentration across China (Fig. 3c). Large PMd_C values (approximately –60 to –30 μg/m^3) were located in the high-polluted NC regions where intensive heavy industries were stopped and the traditional massive social activities and transportations around Chinese New Year were cancelled as part of the COVID-19 quarantine measures. To the south of 30°N, the impacts of the COVID-19 quarantines on the air quality were relatively weaker (–30 ~ 0 μg/m^3) than those in the north. Generally, the south region was less polluted than the north, therefore the baseline of $PM_{2.5}$ concentration was relatively lower (Fig. S4a). In addition, meteorological conditions in the south in February 2020 had no positive contribution (Fig. 3a), which would not lead to the increase of $PM_{2.5}$ concentration. These two possible reasons resulted in a smaller space for $PM_{2.5}$ decrease due to COVID-19 quarantines in the south and accompanying regional differences. To reduce the assessment uncertainties, the percentage of changed $PM_{2.5}$ due to the differences in meteorology were recalculated based on the GEOS-Chem simulations with fixed emission in 1985. As described in the Methods section, the recalculated PMd_C in Figure S6 are consistent with those in Figure 3c, showing a high robustness. Furthermore, the mean $PM_{2.5}$ concentration decreases due to the COVID-19 quarantines in NC, HB and YRD were analyzed, which accounted for 59%, 26% and 72% of the observed February $PM_{2.5}$ concentration in 2020

(Fig. 6).

It should be noted that the sum of PMd_R and PMd_C (i.e., PMd_E) is the total contribution of the emission reduction in February 2020 with respect to 2017 (Fig. 3d). In NC, YRD and HB, the COVID-19 quarantines and routine emission reductions drove $PM_{2.5}$ in the same direction. The mean $PM_{2.5}$ decrease in NC, due to the total emission reduction, was –43.3 $\mu g/m^3$, accounting for 79% of the observed February $PM_{2.5}$ concentration in 2020 (Fig. 6). Although the absolute values of both PMd_R and PMd_C in YRD were smaller than those in NC, the change percentage (92%) was larger because of the lower base $PM_{2.5}$ concentration. In HB, where more than 80% of the confirmed COVID-19 cases in China occurred and the cities were in emergency lockdown, the total anthropogenic emissions were clearly limited, which resulted in a 72% decline in $PM_{2.5}$ in the atmosphere (Fig. 6). In particular, if the anthropogenic emissions did not decline, the $PM_{2.5}$ concentration in NC, YRD and HB would increase to nearly twice the current observation (Fig. 6), indicating significant contributions of human activities to the air pollution in China.

The declines of $PM_{2.5}$ seemed not to be directly proportional to the almost complete shutoff of vehicle traffics and industries, that is, the reduction ratio of $PM_{2.5}$ concentrations were smaller than that of precursor emissions (Wang et al., 2020). The unexpected air pollutions during the marked emission reductions were closely related to the stagnant air flow, enhanced productions of secondary aerosols, and uninterrupted residential heating, power plants and petrochemical facilities (Le et al., 2020). The partial impacts of stagnant meteorological conditions have been explained earlier (Fig. 4). In Wuhan, the $PM_{2.5}$ remained the main pollutant during the city lockdown and the high level of sulphur dioxide (SO_2) may be related to the increased domestic heating and cooking (Lian et al., 2020). In North China, large reductions of primary aerosols were observed, but the decreases in secondary aerosols were much smaller (Sun et al., 2020; Shi et al., 2020). Because of break-off transportations, reduced nitrogen oxide (NO_x) increased the concentrations of ozone and nighttime nitrate (NO_3) radical formations. The increased oxidizing capacity in the atmosphere enhanced the formation of secondary particulate matters (Huang et al., 2020). Thus, the non-linear relationship of emission reduction and secondary aerosols also partially contributed to the haze occurrence during the COVID-19 lockdown.

4 Conclusions and discussion

In the beginning of 2020, the Chinese government implemented top-level emergency response measures to contain the spread of COVID-19. The traditional social activities surrounding Chinese New Year, industrial and transportation activities, etc. were prohibited, which effectively reduced the number of confirmed cases in China. Concomitantly, anthropogenic emissions, which are the fundamental reason for haze pollution, were dramatically reduced by the COVID-19 quarantine measures. In this study, we employed observations and GEOS-Chem simulations to quantify the impacts of the COVID-19 quarantines on the air quality improvement in February 2020 after decomposing the contributions of expected routine emission

reductions and climate variability. Although the specific influences varied by the region, the COVID-19 quarantines substantially decreased the level of haze pollution in the east of China (Fig. 6). In North China, the meteorological conditions were stagnant that enhanced the $PM_{2.5}$ concentration by 30% (relative to the observations in 2020). In contrast, the expected routine emissions reductions and emergency COVID-19 quarantine measures resulted in an 80% decline. In YRD, the impacts of meteorology were negligible but the COVID-19 quarantines decreased $PM_{2.5}$ by 72%. In Hubei Province, the impact of the total emission reduction (72%) evidently exceeded the $PM_{2.5}$ increase due to meteorological conditions (13%). In March, due to the continued control of the COVID-19, the quarantines measures still contributed to the negative anomalies of the observed $PM_{2.5}$ between 2020 and 2017 (Figure 7a). Because the activities in production and life have been gradually resumed in March, the $PM_{2.5}$ drops caused by the COVID-19 quarantines became weaker compared with February (Fig. 7b, c). The contributions of PMd_C to the change of $PM_{2.5}$ concentration in NC, YRD and HB declined from 32.2, 21.0 and 12.1 $\mu g/m^3$ in February to 7.0, 2.4 and 6.7 $\mu g/m^3$ in March respectively.

Because of the common update delay of the emission inventory, we employed a combined analysis consisting of observational and numerical methods. We strictly demonstrated the rationality of this method and the results, mainly based on the relatively constant contribution ratio of changing meteorology from GEOS-Chem simulations under the different emissions (Yin and Zhang 2020). However, there was a certain bias in the simulations by GEOS-Chem model, and the biases also showed regional differences (Dang and Liao, 2019). Therefore, gaps between the assessed results and reality still exist, which requires further numerical experiments when the emission inventory is updated. Furthermore, during the calculation process, the observed $PM_{2.5}$ difference in February 2020 was linearly decomposed into three parts. Although this linear decomposition was reasonable in China in the past few years, we must note that this approximation was lack of considering the meteorology-emission interactions, the product of the emission, the loss lifetime and particularly the sulfate-nitrate-ammonia thermodynamics (Cai et al., 2017), which brought some uncertainties. The actual emission reduction effect is considerable (Fig. 3d), in line with the increasingly strengthened emission reduction policies in recent years. When calculating the PMd_R in 2020, we use the method of extrapolation. Although the result is consistent with others observational and numerical studies (Geng et al., 2020; Zhang et al., 2020; Zhou et al., 2019), it is still conjectures rather than true values. These issues need to be examined in the future studies to unlock respective effects of emissions and meteorological conditions on $PM_{2.5}$ over eastern China. To restrict the possible uncertainties, we set up some constraints: 1. The pivotal contribution ratio of changing meteorology were calculated under two emission levels and recalculated by statistical regressed model; 2. The values of PMd_M and PMd_R were widely compared to previous studies.

If the COVID-19 epidemic did not occurred, the concentrations of $PM_{2.5}$ would increase up to 1.3–1.7 times the observations in February 2020 (Fig. 6). Therefore, the pollution abatement must continue. Because of the huge population base in the east of China, the anthropogenic emissions exceeded the atmospheric environmental capacity even during COVID-19 quarantines. Although the $PM_{2.5}$ dropped much, marked air pollutions also occurred during this unique experiments that the

human emissions were sharply closed. This raised new scientific questions, such as changes of atmospheric heterogeneous reactions and oxidability under extreme emission control, quantitative meteorology-emission interactions, and so on. This also implied reconsiderations of policy for pollution controls and necessity to cut off secondary productions of particulate matters basing on sufficient scientific research (Le et al., 2020; Huang et al., 2020). Some studies estimated that thousands of deaths were prevented during the quarantine because of the air pollution decrease (Chen K. et al., 2020). However, medical systems were still overstressed, and transportation to hospitals also decreased. Furthermore, the deaths related to air pollution were almost all due to respiratory diseases (Wang et al., 2001), and their corresponding medical resources were also further stressed by COVID-19. Therefore, the mortality impacted by the air pollution reduction during the COVID-19 outbreak should be comprehensively assessed in future work.

Data availability. Monthly mean meteorological data are obtained from ERA5 reanalysis data archive: https://cds.climate.copernicus.eu/cdsapp#!/search?type=dataset. $PM_{2.5}$ concentration data are acquired from the China National Environmental Monitoring Centre: http://beijingair.sinaapp.com/. The emissions data of 1985 can be downloaded from http://geoschemdata.computecanada.ca/ExtData/HEMCO/AnnualScalar/, and that of 2010 can be obtained from MIX: http://geoschemdata.computecanada.ca/ExtData/HEMCO/MIX.

Acknowledgements

The National Natural Science Foundation of China (41991283, 9174431 and 41705058), the funding of Jiangsu innovation & entrepreneurship team, and the special project “the impacts of meteorology on large-scale spread of influenza virus” from CIC-FEMD supported this research.

Authors’ contribution

Wang H. J. and Yin Z. C. designed and performed researches. Zhang Y. J. simulated the $PM_{2.5}$ by GEOS-Chem model and Li Y. Y. did the statistical analysis. Yin Z. C. prepared the manuscript with contributions from all co-authors.

Competing interests

The authors declare no conflict of interest.

References

Bey, I., Jacob, D. J., Yantosca, R. M., Logan, J. A., Field, B. D., Fiore, A. M., Li, Q. B., Liu, H. G. Y., Mickley, L. J., and Schultz, M. G.: Global modeling of tropospheric chemistry with assimilated meteorology: Model description and evaluation, J. Geophys. Res. Atmos., 106, 23073–23095, https://doi.org/10.1029/2001jd000807, 2001.

Cai, S., Wang, Y., Zhao, B., Wang S., Chang, X., and Hao, J.: The impact of the "Air Pollution Prevention and Control Action Plan" on $PM_{2.5}$ concentrations in Jing-Jin-Ji region during 2012–2020, Sci. Total Environ., 580, 197 –209, 2017.

Cao, W., Fang, Z., Hou, G., Han, M., Xu X., and Dong, J.: The psychological impact of the COVID-19 epidemic on college students in China, Psychiat. Res., 287, 112934, 2020.

Chen, S., Yang, J., Yang W., Wang, C., and Till, B.: COVID-19 control in China during mass population movements at New Year, Lancet, 395(10226), 764–766, 2020.

Chen, K., Wang, M., Huang, C., Patrick, L., and Paul, T.: Air Pollution Reduction and Mortality Benefit during the COVID-19 Outbreak in China, MedRxiv, https://doi.org/10.1101/2020.03.23.20039842, 2020.

Cleaner air for China, Nat. Geosci., 12, 497–497, https://doi.org/10.1038/s41561-019-0406-7, 2019.

Dang, R., and Liao, H.: Severe winter haze days in the Beijing-Tianjin-Hebei region from 1985 to 2017 and the roles of anthropogenic emissions and meteorology, Atmos. Chem. Phys., 19, 10801–10816, 2019.

Ding, Y., and Liu, Y.: Analysis of long-term variations of fog and haze in China in recent 50 years and their relations with atmospheric humidity, Sci. China Ser. D., 57, 36–46, 2014.

Evans, M. J. and Jacob, D. J.: Impact of new laboratory studies of N_2O_5 hydrolysis on global model budgets of tropospheric nitrogen oxides, ozone, and OH, Geophys. Res. Lett., 32, L09813, https://doi.org/10.1029/2005gl022469, 2005.

Fountoukis, C. and Nenes, A.: ISORROPIA II: a computationally efficient thermodynamic equilibrium model for K^+-Ca^{2+}-Mg^{2+}-NH_4^+-Na^+-SO_4^{2-}-NO_3^--Cl^--H_2O aerosols, Atmos. Chem. Phys., 7, 4639–4659, https://doi.org/10.5194/acp-7-4639-2007, 2007.

Gelaro, R., McCarty, W., Suarez, M. J., Todling, R., Molod, A., Takacs,L., Randles,C.A., Darmenov,A., Bosilovich,M.G., Reichle, R., Wargan, K., Coy, L., Cullather, R., Draper, C., Akella, S., Buchard, V., Conaty, A., da Silva, A. M., Gu, W., Kim, G. K., Koster, R., Lucchesi, R., Merkova, D., Nielsen, J. E., Partyka,G., Pawson,S., Putman,W., Rienecker,M., Schubert,S.D., Sienkiewicz, M., and Zhao, B.: The Modern-Era Retrospective Analysis for Research and Applications, Version 2 (MERRA2), J. Climate, 30, 5419–5454, https://doi.org/10.1175/jcli-d-160758.1, 2017.

Geng, G., Xiao, Q., Zheng, Y., Tong, D., Zhang, Y., Zhang, X., Zhang, Q., He, H., and Liu, Y.: Impact of China's Air Pollution Prevention and Control Action Plan on $PM_{2.5}$ chemical composition over eastern China, Sci. China Ser. D., 62, 1872–1884, https://doi.org/10.1007/s11430-018-9353-x, 2020.

Huang, X., Ding, A., Gao, J., Zheng, B., Zhou, D., Qi, X., Tang, R., Ren, C., Nie, W., Chi, X., Wang, J., Xu, Z., Chen, L., Li, Y., Che, F., Pang, N., Wang, H., Tong, D., Qin, W., Cheng, W., Liu, W., Fu, Q., Chai, F., Davis, S., Zhang, Q., and He, K.: Enhanced secondary pollution offset reduction of primary emissions during COVID-19 lockdown in China, Natl. Sci. Rev., nwaa 137, 2020.

Jacob, D. J.: Heterogeneous chemistry and tropospheric ozone, Atmos. Environ., 34, 2131–2159, https://doi.org/10.1016/s1352- 2310(99)00462-8, 2000.

Kalnay, E., Kanamitsu, M., Kistler, R., Collins, W., Deaven, D., Gandin, L., Iredell, M., Saha, S., White, G.,Woollen, J., Zhu, Y., Leetmaa, A., Reynolds, R., Chelliah, M., Ebisuzaki,W., Higgins, W., Janowiak, J., Mo, K. C., Ropelewski, C.,Wang, J., Jenne, R., and Joseph, D.: The NCEP/NCAR 40-year reanalysis project, B. Am. Meteorol. Soc., 77, 437–471, https://doi.org/10.1175/1520-0477(1996)077<0437:TNYRP>2.0.CO;2, 1996.

Kodros, J. K., Pierce, J. R.: Important global and regional differences in cloud-albedo aerosol indirect effect estimates between simulations with and without prognostic aerosol microphysics, J. Geophys. Res., 122, https://10.1002/2016JD025886, 2017.

Le, T., Wang, Y., Liu, L., Yang, J., Yung, Y. L., Li, G., and John, H.: Unexpected air pollution with marked emission reductions during the covid-19 outbreak in China, Science, 369(6504), eabb7431, 2020.

Li, M., Zhang, Q., Kurokawa, J.-I., Woo, J.-H., He, K., Lu, Z., Ohara, T., Song, Y., Streets, D. G., Carmichael, G. R., Cheng, Y., Hong, C., Huo, H., Jiang, X., Kang, S., Liu, F., Su, H., and Zheng, B.: MIX: a mosaic Asian anthropogenic emission inventory under the international collaboration framework of the MICS-Asia and HTAP, Atmos. Chem. Phys., 17, 935–963, https://doi.org/10.5194/acp-17-935-2017, 2017.

Lian, X., Huang, J., Huang, R., Liu, C., and Zhang, T.: Impact of city lockdown on the air quality of COVID-19-hit of Wuhan city, Sci. Total Environ., 742, 140556, 2020.

Luo, Z.: The impact of new outbreak on economy, capital market and national governance and its response, Finance Economy, 2020(2), 8–15 ,2020.

Ministry of Environmental Protection of China. http://www.mee.gov.cn/xxgk2018/xxgk/xxgk05/201903/t20190306_694550.html, 2019.

Niu, F., Li, Z., Li, C., Lee, K., and Wang, M: Increase of wintertime fog in China: Potential impacts of weakening of the Eastern Asian monsoon circulation and increasing aerosol loading, J. Geophys. Res., 115, D7, 2020.

Park, R.: Natural and transboundary pollution influences on sulfate-nitrate-ammonium aerosols in the United States: Implications for policy, J. Geophys. Res. Atmos., 109, D15204, 2004.

Shi, X., and Brasseur, G.: The Response in Air Quality to the Reduction of Chinese Economic Activities during the COVID Outbreak, Geophys. Res. Lett., 2020, 47, 2020.

Shi, Y., Hu, F., LÜ R., and He, Y.: Characteristics of urban boundary layer in heavy haze process based on beijing 325m tower data, Atmos. Oceanic Sci. Lett., 12, 41–49, 2019.

Song, L., Wang, L., Chen, W., and Zhang, Y.: Intraseasonal Variation of the Strength of the East Asian Trough and Its Climatic Impacts in Boreal Winter, J. Climate, 29 (7), 2557-2577, https://doi.org/10.1175/JCLI-D-14-00834.1, 2016.

Sun, Y., Lei, L., Zhou, W., Chen, C., and Worsnop, D. R.: A chemical cocktail during the COVID-19 outbreak in Beijing, China: Insights from six-year aerosol particle composition measurements during the Chinese New Year holiday. Sci. Total Environ., 140739, 2020.

Thornton, J. A., Jaegle, L., and McNeill, V. F.: Assessing known pathways for HO2 loss in aqueous atmospheric aerosols: Regional and global impacts on tropospheric oxidants, J. Geophys. Res.-Atmos., 113, D05303, https://doi.org/10.1029/2007jd009236, 2008.

Tian, H., Liu, Y., Li, Y., Wu, C., Chen, B., Kraemer, M., Li, B., Cai, J., Xu, B., Yang, Q., Wang, B., Yang, P., Cui, Y., Song, Y., Zheng, P., Wang, Q., Bjornstad, O., Yang, R., Grenfell, B., Pybus, O., Dye, C.: An investigation of transmission control measures during the first 50 days of the COVID-19 epidemic in China, Science, eabb6105, 2020.

Wang, H., and Jin, Y.: The Study on Air Pollution Effects on the Mechanism of Respiratory System. Science of Travel Medicine, 007(002), 29–33, 2001.

Wang, P., Chen, K., Zhu, S., Wang, P., and Zhang, H.: Severe air pollution events not avoided by reduced anthropogenic activities during COVID-19 outbreak, Resour. Conserv. Recy., 158, http://doi:10.1016/j.resconrec.2020.104814, 2020.

Wang, Y., Li, W., Gao, W., Liu, Z., Tian, S., Shen, R., Ji, D., Wang, S., Wang, L., Tang, G., Tao, S., Cheng, M., Wang, G., Gong, Z., Hao, J., and Zhang, Y.: Trends in particulate matter and its chemical compositions in China from 2013–2017, Sci. China Ser. D., 62(12), 1857–1871, 2019.

Xia, J., and Feng, X.: Impacts of COVID-19 epidemic on tourism industry and related countermeasures, Chinese Business and Market, 34(3), 3–10, 2020.

Xiao, D., Li, Y., Fan, S., Zhang, R., Sun, J., and Wang, Y.: Plausible influence of Atlantic Ocean SST anomalies on winter haze in China. Plausible influence of Atlantic Ocean SST anomalies on winter haze in China, Theor. Appl. Climatol., 122, 249–257, 2015.

Yang, Y., Liao, H., and Lou, S.: Increase in winter haze over eastern China in recent decades: Roles of variations in meteorological parameters and anthropogenic emissions, J. Geophys. Res. Atmos., 121, 13050–13065, https://doi.org/10.1002/2016jd025136, 2016.

Yin, Z., and Wang, H.: The relationship between the subtropical Western Pacific SST and haze over North-Central North China Plain, Int. J. Climatol., 36, 3479–3491, 2016.

Yin, Z., and Wang, H.: Role of atmospheric circulations in haze pollution in December 2016, Atmos. Chem. Phys. 17, 11673–11681. https://doi.org/10.5194/acp-17-11673-2017 , 2017.

Yin, Z., Wang, H., and Guo, W.: Climatic change features of fog and haze in winter over North China and Huang-Huai Area, Sci. China Ser. D., 58, 1370–1376, 2015.

Yin, Z., and Zhang, Y.: Climate anomalies contributed to the rebound of $PM_{2.5}$ in winter 2018 under intensified regional air pollution preventions, Sci. Total Environ., 726, 138514, 2020.

Yu, F., and Luo, G.: Simulation of particle size distribution with a global aerosol model: Contribution of nucleation to aerosol and CCN number concentration*s*, Atmos. Chem. Phys., 9, 7691-7710, 2009.

Zhang, X., Xu, X., Ding, Y., Liu, Y., Zhang, H., Wang, Y., Zhong, J.: The impact of meteorological changes from 2013 to 2017 on $PM_{2.5}$ mass reduction in key regions in China, Sci. China Ser. D., 62, 1885–1902, https://doi.org/10.1007/s11430-019-9343-3, 2020.

Zhou, W., Gao, M., He, Y., Wang, Q., Xie, C., Xu, W., Zhao, J., Du, W., Qiu, Y., Lei, L., Fu, P., Wang, Z., Worsnop, D., Zhang, Q., and Sun, Y.: Response of aerosol chemistry to clean air action in Beijing, China: Insights from two-year ACSM measurements and model simulations, Environ. Pollut., 255, 113345, 2019.

Zou, Y., Wang, Y., Zhang, Y., and Koo, J.: Arctic sea ice, Eurasia snow, and extreme winter haze in China, Sci. Adv., 3, e1602751, 2017.

Figure Captions

Figure 1. (a) Variation in existing confirmed cases (bar; red: increase, blue: decrease) and the ratio of accumulated confirmed cases to total confirmed cases (black line) in China. (b) The ratio of work resumption in large industrial enterprises in the east of China. (c) Time of the official 7-days holiday of Chinese New Year from 2013 to 2020.

Figure 2. Differences in the observed $PM_{2.5}$ (unit: μg/m^3) in February between 2020 and 2017. The black boxes indicate the locations of North China (NC, 32.5-42°N,110-120°E), the Yangtze River Delta (YRD, 28-32.5°N,118-122°E) and Hubei Province (HB, 30-32.5°N,109.5-116°E).

Figure 3. $PM_{2.5}$ difference (unit: μg/m^3) in February between 2020 and 2017 due to (a) changing meteorology (PMd_M), (b) expected routine emission reductions (PMd_R), (c) the COVID-19 quarantines (PMd_C), and (d) due to the total emission reduction ($PMd_E = PMd_R + PMd_C$).

Figure 4. Differences in the observed atmospheric circulation in February between 2020 and 2017, including (a) geopotential potential height at 500 hPa (unit: gpm), (b) wind at 850 hPa (arrows; unit: m/s), surface relative humidity (shading; unit: %). The atmospheric circulations in the stagnant days (e.g., from 8–13 and 19–25 February 2020) were also showed, including (c) geopotential potential height at 500 hPa (shading; unit: gpm) and its climate mean in February (contour), and (d) wind at 850 hPa (black arrows; unit: m/s), its climate mean (blue arrows) and the increased surface relative humidity (shading; unit: %, stagnant days minus climate mean).

Figure 5. Variation in PMd_R (unit: μg/m^3) with respect to the February 2017 level in Beijing, Shanghai and Wuhan from 2015 to 2019. PMd_R in 2020 was linearly extrapolated from that in the 2015–2019 period. The dotted line is the linear trend.

Figure 6. Contributions of PMd_M (orange bars with hatching), PMd_R (purple bars with hatching) and PMd_C (blue bars with hatching) to the change in $PM_{2.5}$ concentration (unit: μg/m^3) between 2020 and 2017 in the three regions. The observed $PM_{2.5}$ concentration in February 2017 (black) and 2020 (gray) was also plotted, and the expected $PM_{2.5}$ concentration without the COVID-19 quarantine is indicated by black hollow bars. The contribution ratios of the three factors (relative to the $PM_{2.5}$ observations in 2020) are also indicated on the corresponding bars.

Figure 7. (a) Differences in the observed $PM_{2.5}$ (unit: μg/m3) in March between 2020 and 2017. (b) Contributions of PMd_C to the change in $PM_{2.5}$ concentration (unit: μg/m^3) between 2020 and 2017 and (c) the contribution ratios of PMd_C (relative to the $PM_{2.5}$ observations in 2020) in March (blue) and February (red) in the three regions.

Figures

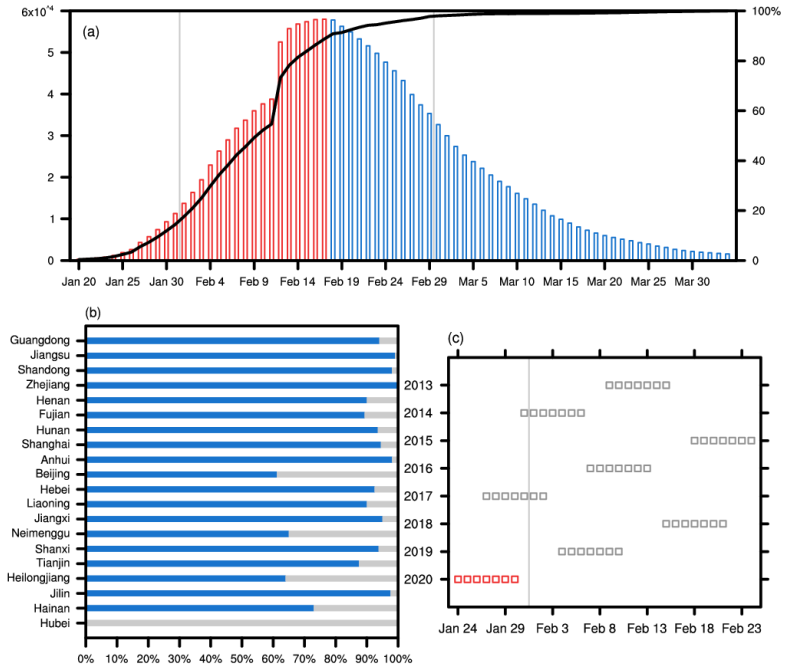

Figure 1. (a) Variation in existing confirmed cases (bar; red: increase, blue: decrease) and the ratio of accumulated confirmed cases to total confirmed cases (black line) in China. (b) The ratio of work resumption in large industrial enterprises in the east of China. (c) Time of the official 7-days holiday of Chinese New Year from 2013 to 2020.

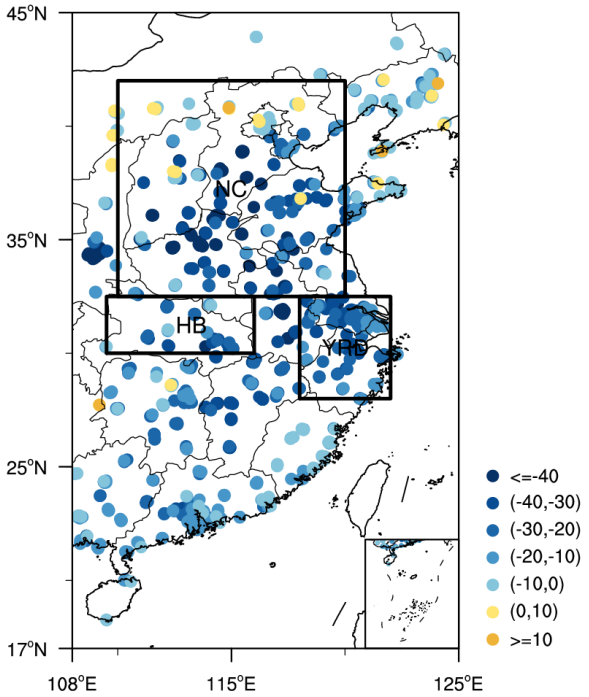

Figure 2. Differences in the observed $PM_{2.5}$ (unit: μg/m^3) in February between 2020 and 2017. The black boxes indicate the locations of North China (NC, 32.5-42°N,110-120°E), the Yangtze River Delta (YRD, 28-32.5°N,118-122°E) and Hubei Province (HB, 30-32.5°N,109.5-116°E).

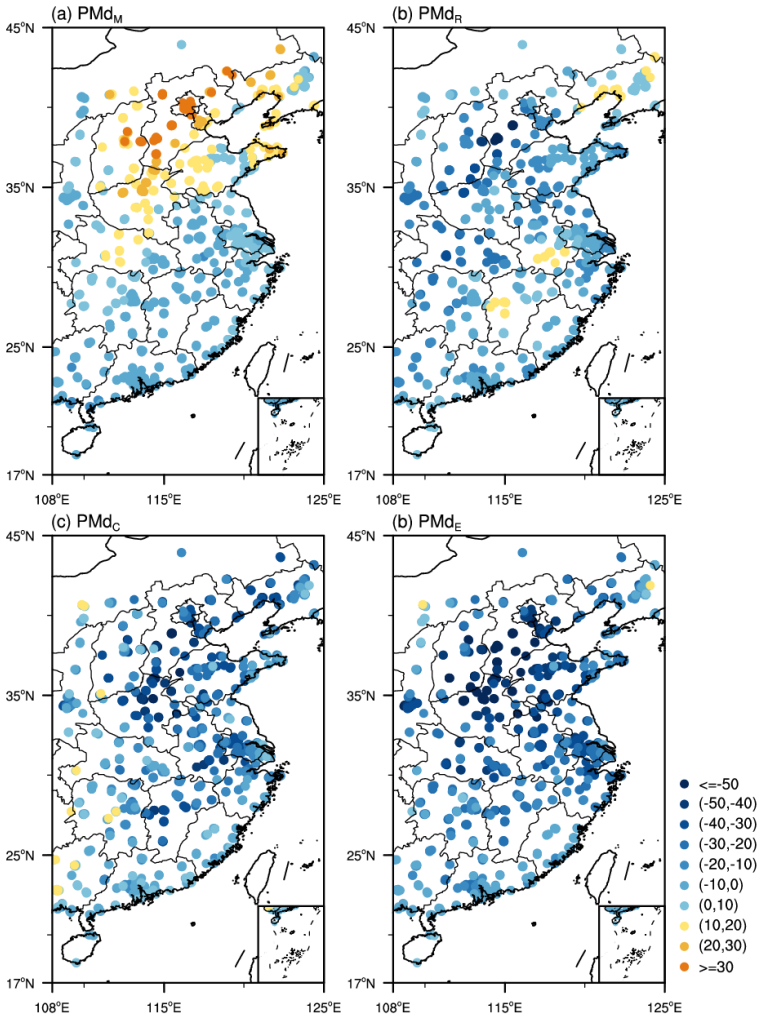

Figure 3. $PM_{2.5}$ difference (unit: μg/m^3) in February between 2020 and 2017 due to (a) changing meteorology (PMd_M), (b) expected routine emission reductions (PMd_R), (c) the COVID-19 quarantines (PMd_C), and (d) due to the total emission reduction ($PMd_E = PMd_R + PMd_C$).

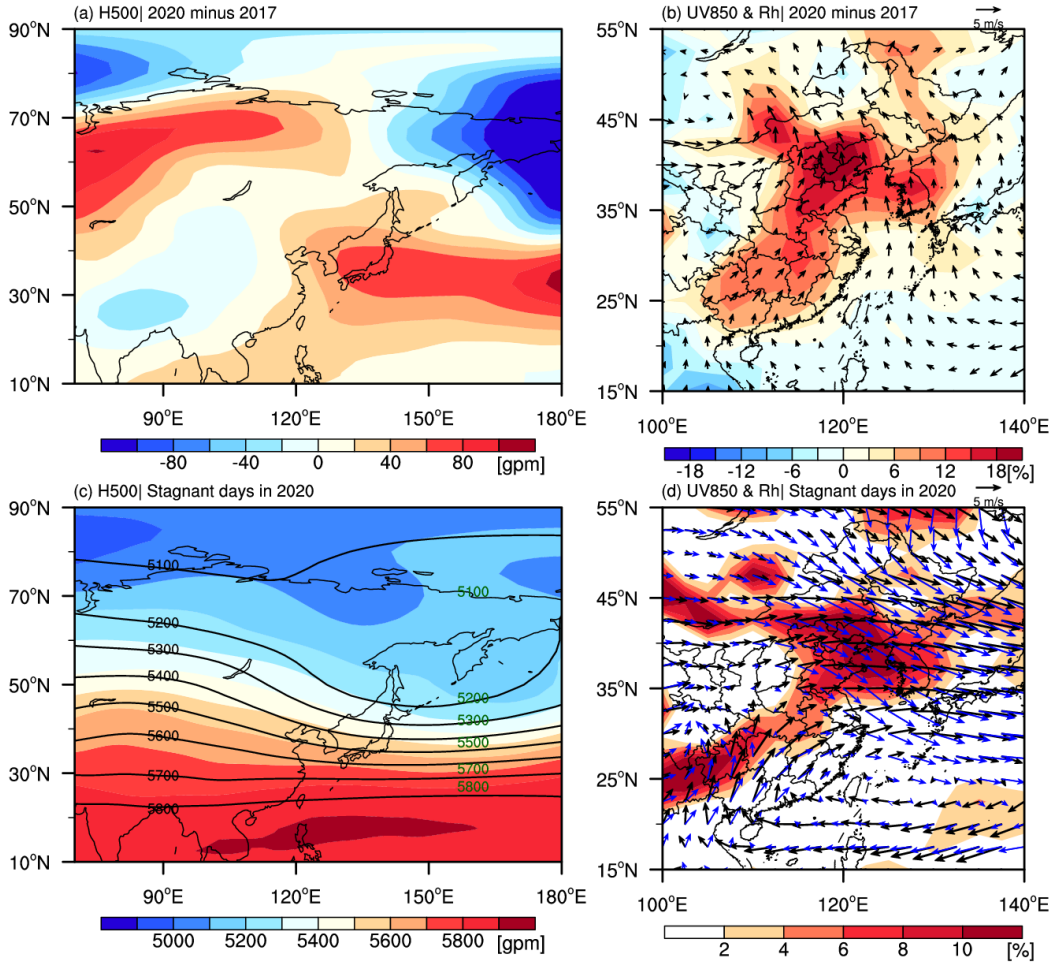

476

477 **Figure 4.** Differences in the observed atmospheric circulation in February between 2020 and 2017, including (a) geopotential
478 potential height at 500 hPa (unit: gpm), (b) wind at 850 hPa (arrows; unit: m/s), surface relative humidity (shading; unit: %).
479 The atmospheric circulations in the stagnant days (e.g., from 8–13 and 19–25 February 2020) were also showed, including (c)
480 geopotential potential height at 500 hPa (shading; unit: gpm) and its climate mean in February (contour), and (d) wind at 850
481 hPa (black arrows; unit: m/s), its climate mean (blue arrows) and the increased surface relative humidity (shading; unit: %,
482 stagnant days minus climate mean).

483

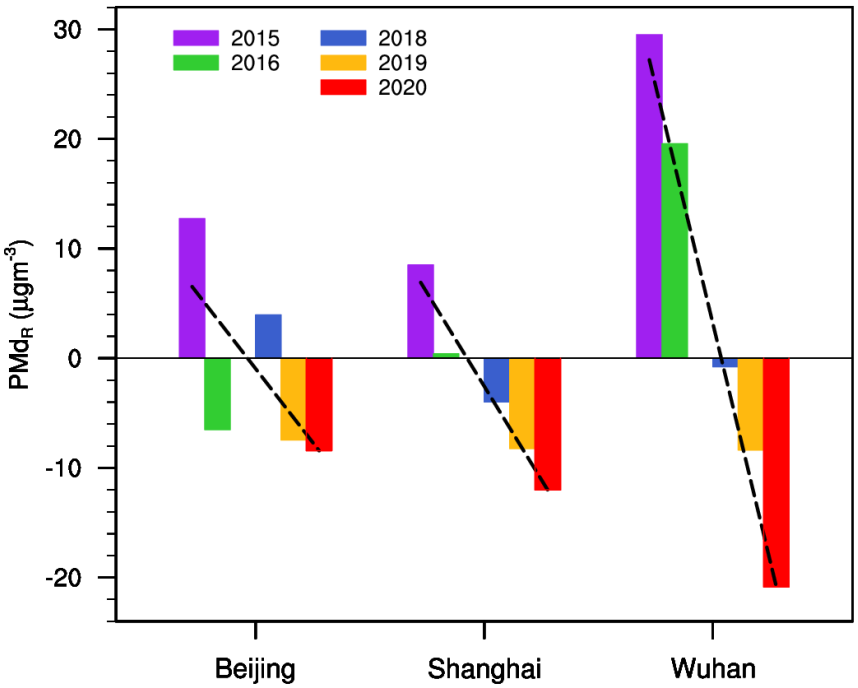

Figure 5. Variation in PMd_R (unit: μg/m^3) with respect to the February 2017 level in Beijing, Shanghai and Wuhan from 2015 to 2019. PMd_R in 2020 was linearly extrapolated from that in the 2015–2019 period. The dotted line is the linear trend.

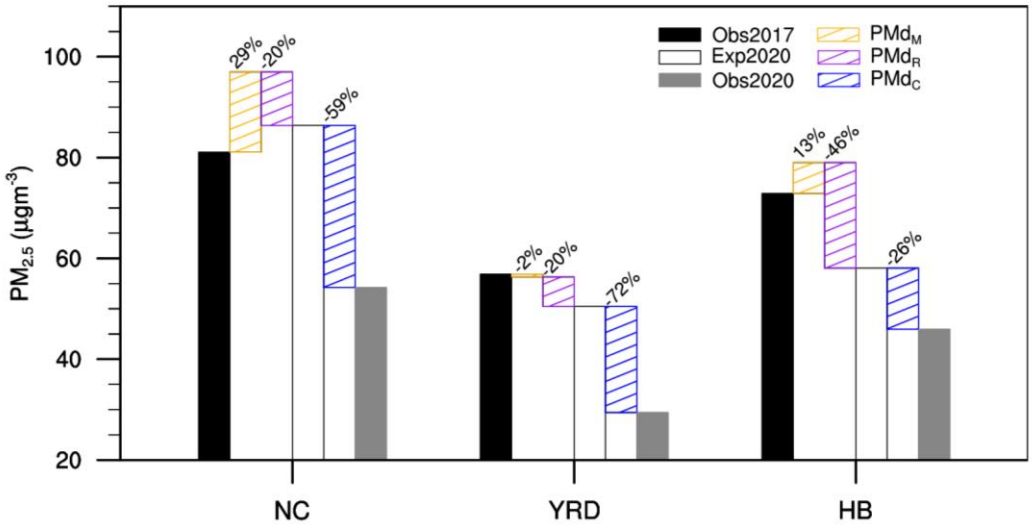

Figure 6. Contributions of PMd_M (orange bars with hatching), PMd_R (purple bars with hatching) and PMd_C (blue bars with hatching) to the change in $PM_{2.5}$ concentration (unit: μg/m^3) between 2020 and 2017 in the three regions. The observed $PM_{2.5}$ concentration in February 2017 (black) and 2020 (gray) was also plotted, and the expected $PM_{2.5}$ concentration without the COVID-19 quarantine is indicated by black hollow bars. The contribution ratios of the three factors (relative to the $PM_{2.5}$ observations in 2020) are also indicated on the corresponding bars.

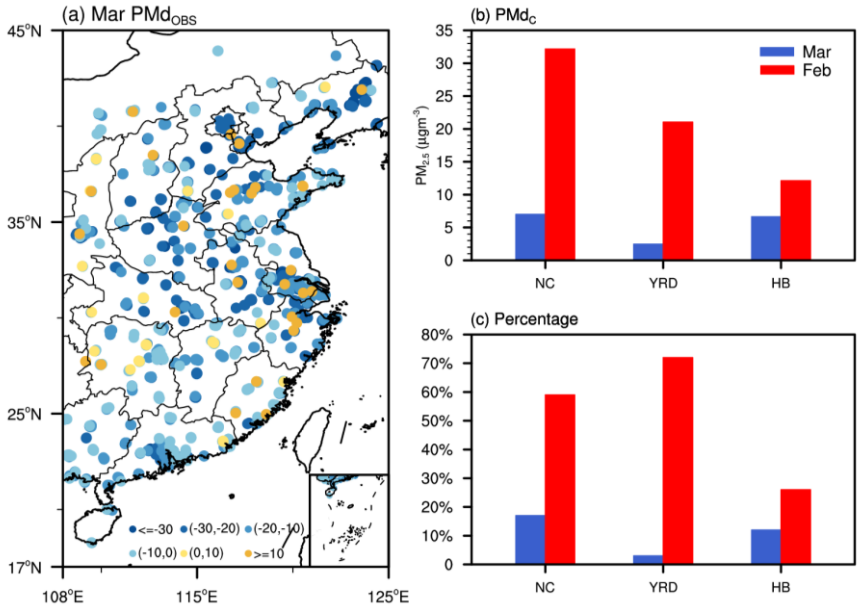

494

495 **Figure 7.** (a) Differences in the observed $PM_{2.5}$ (unit: μg/m^3) in March between 2020 and 2017. (b) Contributions of PMd_C to

496 the change in $PM_{2.5}$ concentration (unit: μg/m^3) between 2020 and 2017 and (c) the contribution ratios of PMd_C (relative to the

497 $PM_{2.5}$ observations in 2020) in March (blue) and February (red) in the three regions.

498

499